

Modern Physics Letters B
 © World Scientific Publishing Company

Charge instabilities of the extended attractive Hubbard Model on the cubic lattice

Raymond Frésard

*Normandie Univ, ENSICAEN, UNICAEN, CNRS, CRISMAT, 14050 Caen, France
 Raymond.Fresard@ensicaen.fr*

Vu Hung Dao

*Normandie Univ, ENSICAEN, UNICAEN, CNRS, CRISMAT, 14050 Caen, France
 vu-hung.dao@ensicaen.fr*

Received (Day Month Year)

Revised (Day Month Year)

The paramagnetic phase of the extended attractive Hubbard model on the cubic lattice is studied within the spin rotation invariant Kotliar-Ruckenstein slave-boson representation at zero temperature. It is obtained that the quasiparticle residue of the Fermi liquid phase vanishes for all densities at an interaction strength slightly smaller than U_c that signals the Brinkman-Rice transition, and that it weakly depends on density. While for vanishing non-local interaction parameters homogeneous static charge instabilities are found in a rather narrow window centered around quarter filling and $U \simeq 0.8 U_c$, increasing them to $V = -0.2 U$ results into a severe narrowing of this window. On the contrary, when all interaction parameters are attractive, for example for $V = 0.2 U$, a large parameter range in which homogeneous static charge instabilities is found. Yet, this systematically happens inside the Fermi liquid phase.

Keywords: Hubbard model; slave boson; charge instabilities.

1. Introduction

While the Hubbard model has been originally introduced to describe metallic magnetism,¹⁻³ it gained renewed interest after Anderson's proposal that it represents a minimal model for the d electrons within the CuO_2 layers common to the high T_c superconductors.⁴ Yet, it is fair to say that this model still lacks a broadly accepted solution, especially in the strongly correlated regime, despite its apparent simplicity following from its assumption that the non-local Coulomb interaction is fully screened but locally. More recently, it has been proposed that non-local interactions are of relevance, too, especially in the context of two-dimensional systems such as surface systems,⁵ graphene,⁶ transition metal dichalcogenides,⁷ ultracold fermions in optical lattices,⁸⁻¹⁰ and correlation induced capacitance enhancement.¹¹

While the local interaction is repulsive in most instances, attractive interaction has been invoked in ultracold fermion experiments¹² and also in the condensed

matter context^{13,14} and received strong interest.^{15–18} In particular, in the locally repulsive but non-locally attractive case, phase separation into a high and low density state has been reported.^{11,19}

The purpose of this work is to establish the influence of an attractive local interaction on this instability in general, and on the Landau Fermi liquid parameter F_0^s in particular. We hence focus on the extended nondegenerate Hubbard model which describes the simplest correlated metals and investigate the influence of intersite Coulomb on the charge instabilities. Thereby we follow the route initiated by Vollhardt²⁰ who investigated Landau Fermi liquid parameters F_0^a and F_0^s for ^3He . Further studies gave the Fermi liquid interaction and the quasiparticle scattering amplitude on the Fermi surface in ^3He .²¹

Since we are also interested in the strongly correlated regime we perform our investigations in a framework which is able to capture interaction effects beyond the physics of Slater determinants. It is an extension of the Kotliar and Ruckenstein slave boson representation that reproduced the Gutzwiller approximation on the saddle-point level²² and entails the interaction driven Brinkman-Rice metal-to-insulator transition.²³ A whole range of valuable results have been obtained with Kotliar and Ruckenstein²² and related^{24,25} slave boson representations which motivate the present study. In particular they have been used to describe antiferromagnetic,²⁶ ferromagnetic,²⁷ spiral^{28–30} and striped^{31–34} phases. Furthermore, the competition between the latter two has been addressed as well.³⁵ Besides, it has been obtained that the spiral order continuously evolves to the ferromagnetic order in the large U regime ($U \gtrsim 60t$)²⁷ so that it is unlikely to be realized experimentally. Consistently, in the two-band model, ferromagnetism was found as a possible groundstate only in the doped Mott insulating regime.³⁶ Yet, adding a ferromagnetic exchange coupling was shown to bring the ferromagnetic instability line into the intermediate coupling regime.³⁷ A similar effect has been obtained with a sufficiently large next-nearest-neighbor hopping amplitude³⁸ or going to the fcc lattice.³⁹ The influence of the lattice geometry on the metal-to-insulator transition was discussed, too.⁴⁰ For instance, a very good agreement with Quantum Monte Carlo simulations on the location of the metal-to-insulator transition for the honeycomb lattice has been demonstrated.⁴¹ Finally, further motivation comes from the strongly inhomogeneous polaronic states that have been found in correlated heterostructures using the Hubbard model extended with intersite Coulomb interactions.⁴²

Furthermore, comparison of ground state energies to existing numerical solutions have been carried out for the square lattice, too. For instance, for $U = 4t$ it could be shown that the slave boson ground state energy is larger than its counterpart by less than 3%.²⁸ For larger values of U , it has been obtained that the slave boson ground state energy exceeds the exact diagonalization data by less than 4% (7%) for $U = 8t$ ($20t$) and doping larger than 15%. The discrepancy increases when the doping is lowered.³⁰ It should also be emphasized that quantitative agreement to

quantum Monte Carlo charge structure factors was established.⁴³

The purpose of this paper is to evaluate the Fermi liquid Landau parameter F_0^s for the metallic state in the extended Hubbard model in the case where the local interaction is attractive. This extends earlier work on the locally repulsive case¹⁹ that lead to electronic phase separation which may considerably enhance the capacitance of capacitors when their metallic plates are strongly correlated.¹¹

2. Extended Hubbard model

Numerous studies of correlated electrons have been devoted to the properties of the Hubbard model on a square lattice, especially after Anderson's proposal that it represents a minimal model for the d electrons within the CuO_2 layers common to the high T_c superconductors.⁴ Yet the Hubbard model assumes a perfect screening of the long-range part of the Coulomb interaction. This may be questionable and the relevance of this approximation may be assessed by considering the extended Hubbard model that reads:

$$H = \sum_{i,j,\sigma} t_{ij} c_{i\sigma}^\dagger c_{j\sigma} + U \sum_i n_{i\uparrow} n_{i\downarrow} + \frac{1}{2} \sum_{i,j} V_{ij} n_i n_j \quad (1)$$

and includes intersite Coulomb V_{ij} interactions. These elements decay fast with increasing distance $|\vec{R}_i - \vec{R}_j|$, but extend in general beyond nearest neighbors. Here $c_{i\sigma}^\dagger$ are electron creation operators at site i with spin σ , and $n_{i\sigma} = c_{i\sigma}^\dagger c_{i\sigma}$. We consistently use the particle-hole symmetric form for both density-density interaction terms. Although one expects that $V_{ij} > 0$, in certain cases effective intersite Coulomb interactions may be attractive.¹⁴ Therefore, we shall treat $\{V_{ij}\}$ as effective parameters and consider both signs of them below.

We perform our calculations in the spin rotation invariant formulation of the Kotliar-Ruckenstein slave boson representation of the Hubbard model.^{22, 25, 37} Though such functional integrals can be calculated exactly for the Ising chain⁴⁴ and some toy models,⁴⁵ even with the Kotliar and Ruckenstein representation,^{46, 47} this is unpractical on higher dimensional lattice. Here we rather resort to a calculation at one-loop order around the paramagnetic saddle-point. This saddle-point approximation is exact in the large degeneracy limit, and the Gaussian fluctuations provide the $1/N$ corrections.²⁵ Moreover it obeys a variational principle in the limit of large spatial dimensions where the Gutzwiller approximation becomes exact for the Gutzwiller wave function.⁴⁸⁻⁵⁰ Furthermore, it could be shown in this limit that longer ranged interactions are not dynamical and reduce to their Hartree approximation.⁵¹ Therefore, our approach also obeys a variational principle in this limit when applied to the above extended Hubbard model Eq. (1). All used formulas may be found in Lhoutellier et. al.'s work.³⁷

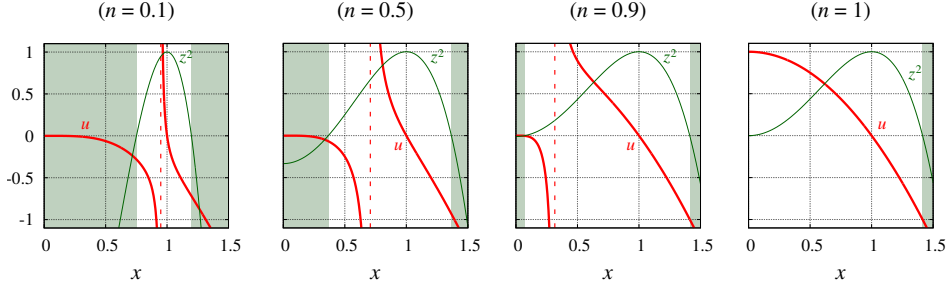
4 *R. Frésard and V. H. Dao*


Fig. 1. Saddle-point function u (red, thick line) and renormalization factor z^2 (green, thin line) as functions of x , for different electron densities. The shaded area corresponds to unphysical values of x yielding $z^2 < 0$.

3. Saddle-point solutions

In the translational invariant paramagnetic phase, all local quantities are site independent. The saddle-point values of the boson fields representing the atomic states with respectively zero, single and double occupancy may be expressed as

$$e = \frac{x^2 + \delta}{2x}, \quad p_0 = \sqrt{1 - \frac{x^4 + \delta^2}{2x^2}}, \quad d = \frac{x^2 - \delta}{2x}, \quad (2)$$

where the doping from half-filling is $\delta = 1 - n$, n is the electron density, and the variable $x = e + d$. Hence the auxiliary boson fields obey the physical constraints on average :

$$e^2 + p_0^2 + d^2 = 1, \quad \text{and} \quad p_0^2 + 2d^2 = 1 - \delta. \quad (3)$$

The value of x is determined by solving the saddle-point equation^{25, 52, 53}

$$u(x) \equiv \frac{(1 - x^2)x^4}{x^4 - \delta^2} = \frac{U}{U_0}. \quad (4)$$

Here we have introduced the coupling scale

$$U_0 = -\frac{8}{1 - \delta^2} \tilde{\varepsilon} \quad (5)$$

where $\tilde{\varepsilon}$ is the averaged kinetic energy. Here we do not attempt to unravel the richness arising at finite temperature as known in the repulsive case,^{41, 53, 54} but we instead stick to zero temperature. Remarkably, the intersite interaction $V_{i,j}$ does not enter Eq. (4). In the paramagnetic phase, it only influences the fluctuations, and does not change the electron localization driven by the strong onsite interaction U .

The saddle-point equation can have zero, one, or two solutions, depending on the onsite Coulomb interaction and the density. The function $u(x)$ is plotted in Fig. 1 for different values of the density, together with the inverse-mass renormalization factor

$$z^2 = \frac{2p_0^2(e + d)^2}{1 - \delta^2} = 1 - \frac{(1 - x^2)^2}{1 - \delta^2}. \quad (6)$$

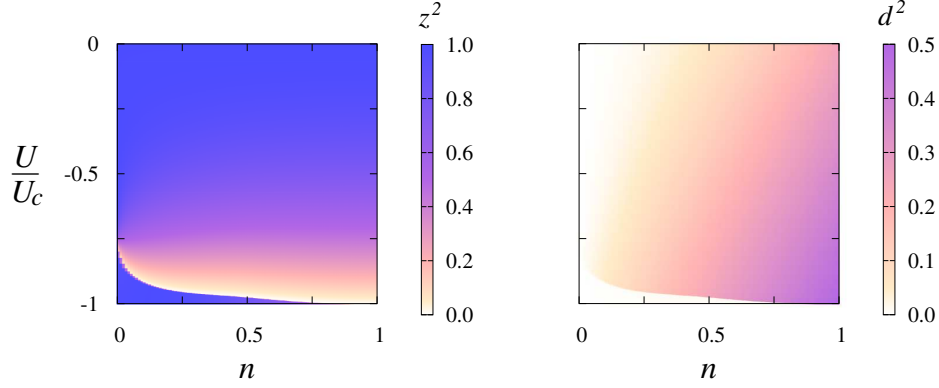


Fig. 2. (left) The inverse-mass renormalization factor z^2 and (right) the saddle-point value of the double occupancy d^2 , as functions of the density n and the onsite Coulomb interaction U .

In the case of a positive U there is at most one solution. For a finite doping the function $u(x)$ diverges at $x = \sqrt{|\delta|}$, so the saddle-point equation always possesses one solution, however large U is. But at half-filling, $u(x) = 1 - x^2$. As a consequence, the solution exists only below a critical value $U_c = \lim_{\delta \rightarrow 0} U_0 = -8\tilde{\epsilon}$. For the presently investigated 3D cubic lattice $U_c = 16.0387t$. At this coupling the Brinkman-Rice transition occurs from a metallic state to a Mott insulator. Indeed the effective mass diverges as z^2 vanishes at $x = 0$ for $U = U_c$, as shown in Fig. 1.

For a negative U the saddle-point equation can have two solutions. But some of them yield $z^2 < 0$ and, thus, are not physical. The allowed values are restricted to the range $\sqrt{1 - \sqrt{1 - \delta^2}} \leq x \leq \sqrt{1 + \sqrt{1 - \delta^2}}$. At half-filling, mirroring the positive U situation, there is a single solution, which is relevant only for $|U| < U_c$. At the critical coupling, the effective mass diverges and a transition into an insulating state takes place. Beyond, the values $x > \sqrt{2}$ are not physical. At density $n < 1$, the saddle-point equation possesses two solutions : $x_- < \sqrt{|\delta|}$ and $x_+ > \sqrt{|\delta|}$. When x_+ is allowed, it is the saddle-point solution with the lowest free energy : it yields the largest double occupancy d^2 (hence the lowest interaction energy), and often, the largest z^2 (hence the lowest kinetic energy) as well. Similarly to the half-filling case, the solution x_+ is not physical for $|U|$ larger than a critical coupling \tilde{U}_c . The latter decreases from U_c at half-filling to $U_0/2$ at $n = 0$. As shown in Fig. 2, the renormalization factor z^2 decreases from unity at $U = 0$ to zero at the critical coupling. Along the line $\tilde{U}_c(n)$ the paramagnetic state described by the solution x_+ is an incoherent insulator. For $|U| > \tilde{U}_c$, only the solution x_- is possible. However the latter yields a vanishingly small value of d^2 (see Fig. 2). One can then doubt the relevance of this saddle-point solution, because one would expect that the attractive onsite interaction should favor the double occupancy. Since no plausible homogeneous phase may be stabilized, one should seek for inhomogeneous ones,

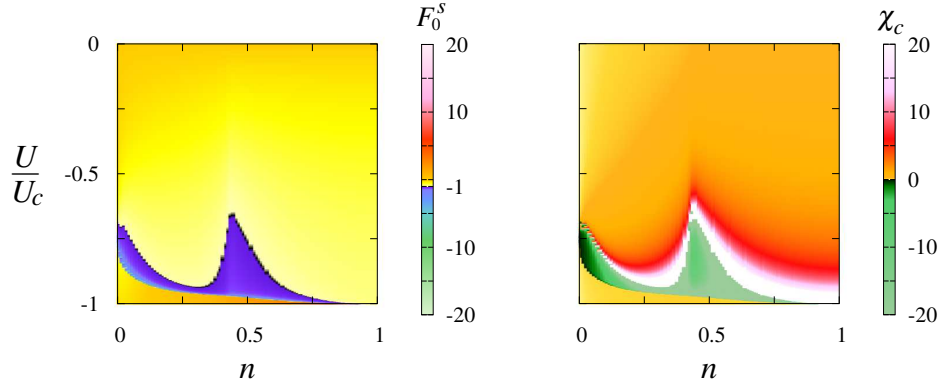
6 *R. Frésard and V. H. Dao*


Fig. 3. (left) Landau parameter F_0^s and (right) static homogeneous charge susceptibility χ_c for $V = 0$, as functions of density n and onsite Coulomb interaction U . The white shade corresponds to values larger than 20.

which however is outside the scope of the present work. We will not discuss further the solution x_- since, as shown below, the uniform paramagnetic state is already unstable for values of $|U|$ smaller than the critical coupling.

4. Charge instabilities

The stability of the paramagnetic state obtained in the previous section is investigated by means of the symmetric Landau Fermi-liquid parameter F_0^s and the static charge response function χ_c in the long wavelength limit. The latter quantities are numerically calculated within the one-loop approximation. For the present discussion, we consider an isotropic intersite Coulomb interaction restricted to the nearest neighbor sites, with $V_{ij} = V$.

Figs. 3–5 display the variations of F_0^s and χ_c , as functions of the density n and the onsite interaction U , for respectively $V = 0$, $V = -0.2 U$, and $V = 0.2 U$. The shades in the graphics have been chosen to highlight the loci in the parameter space where $F_0^s = -1$. The values slightly larger than -1 are plotted with a light yellow hue, in contrast to the values slightly lower than -1 plotted with a dark blue hue. The value $F_0^s < -1$ results in a charge response $\chi_c < 0$ (plotted with a green shade), which indicates an instability of the paramagnetic solution.

For an attractive onsite coupling, without intersite interaction (see Fig. 3), the uniform paramagnetic state is unstable in a narrow two-dimensional parameter space centered around quarter filling and $U \simeq 0.8 U_c$. Note that the instability arises within the region of existence of the saddle-point solution x_+ , at values of $|U| < \tilde{U}_c$ well inside the Fermi liquid phase.

When a repulsive intersite interaction is turned on, the narrow window of instability rapidly shrinks down to the vicinity of a critical point located at $n = 0$ and

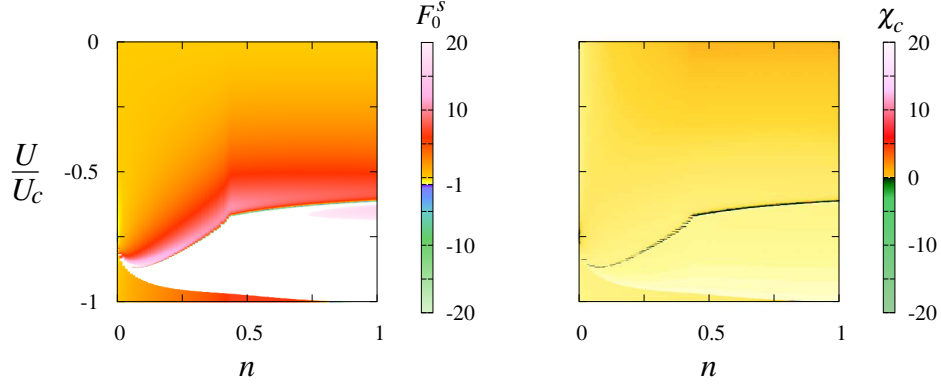


Fig. 4. (left) Landau parameter F_0^s and (right) static homogeneous charge susceptibility χ_c for $V = -0.2 U$, as functions of density n and onsite Coulomb interaction U . The white shade corresponds to values larger than 20.

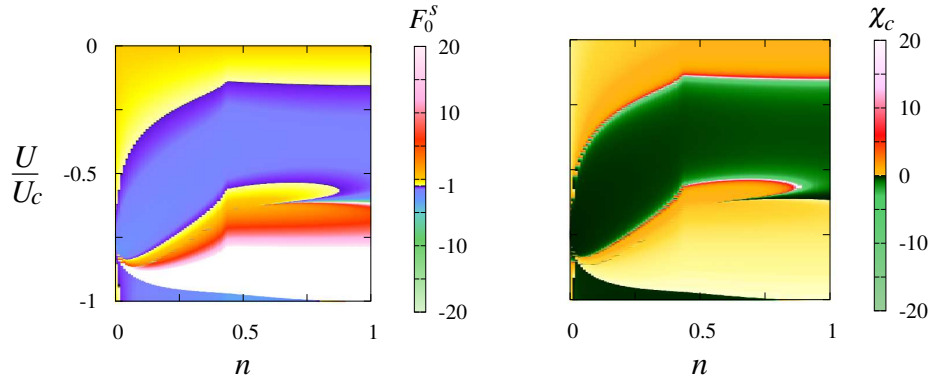


Fig. 5. (left) Landau parameter F_0^s and (right) static homogeneous charge susceptibility χ_c for $V = 0.2 U$, as functions of density n and onsite Coulomb interaction U . The white shade corresponds to values larger than 20.

$U = -0.5 U_0$. However, as shown in Fig. 4, a second region of instability emerges in the form of a line where F_0^s diverges. The line of instability is located inside the Fermi liquid phase.

When both the onsite and intersite interactions are attractive, the two-dimensional region of instability grows and is displaced towards lower values of $|U|$ (see Fig. 5). The line of instability is also present. We have noted that the location of this line seems not to depend on the sign of the intersite interaction.

5. Discussion and summary

Summarizing, we have investigated the paramagnetic phase of the extended attractive Hubbard model on the cubic lattice within the spin rotation invariant Kotliar-Ruckenstein slave-boson representation, first on the saddle-point level, and second at one-loop order. The saddle-point equations may be cast into a single algebraic equation,^{25,52} independent of the non-local interaction parameters.³⁷ In the repulsive case, it reproduces the Brinkman-Rice metal-to-insulator transition at half-filling. Despite the multiple solutions of the saddle-point equations no phase transition is found away from half-filling, regardless of whether the density or the interaction strength is varied (at zero temperature). In the attractive case we found the situation to be qualitatively different, with a first order transition for any density when increasing $-U$ from a Fermi liquid phase to a marginally relevant one. In fact, the phase boundary is given by the line where the effective mass diverges or, in other words, where the quasiparticle residue vanishes.

We then turned to the Landau parameter F_0^s and, in particular, to its dependence on the non-local interaction parameters. Again, we obtain results that qualitatively differ from the repulsive case. Of course, the nature of the instabilities differs, but one may wish to unify their discussion. Intuitively, while one here expects some form of charge (pair) density wave, the repulsive model naturally yields magnetic instabilities/orderings. In particular, for a given density, the Landau parameter F_0^a may reach -1 at a critical value of the interaction strength, and remains smaller than -1 for all values of the interaction strength larger than the critical one. This is indeed yielded by the calculation.⁵⁵ That does not prove that the ground state is ferromagnetic, as these instabilities compete with incommensurate ones. And, indeed, a ferromagnetic ground state could at best be stabilized for very large U and small doping,²⁷ in agreement with Nagaoka ferromagnetism. Nevertheless, for a given point in the phase diagram, $F_0^a < -1$ remains a rather reliable indicator of a magnetic instability. In contrast, for the attractive cases studied here, the obtained behavior of F_0^s differs qualitatively. For instance, for vanishing non-local interaction parameters, we found $F_0^s < -1$ in a rather narrow window centered around quarter filling and $U \simeq 0.8 U_c$. This window is even far narrower for $V = -0.2 U$ and is shifted towards smaller values of $|U|$. In fact, the expected pair density wave is not signaled by homogeneous instabilities. Hence, contrary to the repulsive model, $F_0^s < -1$ does not turn out to be a good indicator of incommensurate pair density wave instabilities, which determination remains as a task for future work.

Acknowledgments

R.F. is grateful for the warm hospitality at MPI Stuttgart where part of this work has been done.

References

1. J. Hubbard, *Proc. R. Soc. London* **A276** (1963) 238.

2. M. C. Gutzwiller, *Phys. Rev. Lett.* **10** (1963) 159.
3. J. Kanamori, *Prog. Theor. Phys.* **30** (1963) 275.
4. P. W. Anderson, *Science* **235** (1987) 1196.
5. P. Hansmann, T. Ayrál, L. Vaugier, P. Werner, and S. Biermann, *Phys. Rev. Lett.* **110** (2013) 166401.
6. M. Schüler, M. Rösner, T. O. Wehling, A. I. Lichtenstein, and M. I. Katsnelson, *Phys. Rev. Lett.* **111** (2013) 036601.
7. E. G. C. P. van Loon, M. Rösner, G. Schönhoff, M. I. Katsnelson, and T. O. Wehling, *npj Quantum Materials* **3** (2018) 32.
8. O. Dutta O, T. Sowinski, and M. Lewenstein, *Phys. Rev.* **A87** (2013) 023619.
9. O. Dutta, M. Gajda, P. Hauke, M. Lewenstein, D. S. Lühmann, B. A. Malomed, T. Sowinski, and J. Zakrzewski, *Reports on Progress in Physics* **78** (2015) 066001.
10. E. G. C. P. van Loon, M. I. Katsnelson, and M. Lemeshko *Phys. Rev.* **B92** (2015) 081106.
11. K. Steffen, R. Frésard, and T. Kopp, *Phys. Rev.* **B95** (2017) 035143.
12. T. Esslinger, *Annual Review of Condensed Matter Physics* **1** (2010) 129.
13. D. van der Marel and G. A. Sawatzky, *Phys. Rev.* **B37** (1988) 10674.
14. R. Micnas, J. Ranninger, and S. Robaszkiewicz, *Rev. Mod. Phys.* **62** (1990) 113.
15. E. G. C. P. van Loon and M. I. Katsnelson, Proc. of XXIXth IUPAP Conference on Computational Physics CCP2017, *J. Phys.: Conf. Series* **1136** (2018) 012006.
16. A. Amaricci, A. Camjayi, K. Haule, G. Kotliar, D. Tanaskovic, and V. Dobrosavljevic, *Phys. Rev.* **B82** (2010) 155102.
17. T. Ayrál, S. Biermann, and P. Werner, *Phys. Rev.* **B87** (2013) 125149.
18. H. Terletska, T. Chen, and E. Gull, *Phys. Rev.* **B95** (2017) 115149.
19. R. Frésard, K. Steffen, and Th. Kopp, Proc. of the 18th International Conference on Recent Progress in Many-Body Theories (MBT18), Niagara Falls (2015), *J. Phys.: Conf. Series* **702** (2016) 012003.
20. D. Vollhardt, *Rev. Mod. Phys.* **56** (1984) 99.
21. M. Pfizner and P. Wölfle, *Phys. Rev.* **B33** (1986) 2003.
22. G. Kotliar and A. E. Ruckenstein, *Phys. Rev. Lett.* **57** (1986) 1362.
23. W. F. Brinkman and T. M. Rice, *Phys. Rev.* **B2** (1970) 4302.
24. T. C. Li, P. Wölfle, and P. J. Hirschfeld, *Phys. Rev.* **B40** (1989) 6817.
25. R. Frésard and P. Wölfle, *Int. J. of Mod. Phys.* **B6** (1992) 685; **B6** (1992) 3087.
26. L. Lilly, A. Muramatsu, and W. Hanke, *Phys. Rev. Lett.* **65** (1990) 1379.
27. B. Möller, K. Doll, and R. Frésard, *J. Phys.: Condensed Matter* **5** (1993) 4847.
28. R. Frésard, M. Dzierzawa, and P. Wölfle, *Europhys. Lett.* **15** (1991) 325.
29. E. Arrigoni and G. C. Strinati, *Phys. Rev.* **B44** (1991) 7455.
30. R. Frésard and P. Wölfle, *J. Phys.: Condensed Matter* **4** (1992) 3625.
31. G. Seibold, E. Sigmund, and V. Hizhnyakov, *Phys. Rev.* **B57** (1998) 6937.
32. J. Lorenzana and G. Seibold, *Phys. Rev. Lett.* **89** (2002) 136401; **90** (2003) 066404; **94** (2005) 107006.
33. M. Raczkowski, R. Frésard, and A. M. Oleś, *Phys. Rev.* **B73** (2006) 174525.
34. M. Raczkowski, M. Capello, D. Poilblanc, R. Frésard, and A. M. Oleś, *Phys. Rev.* **B76** (2007) 140505(R).
35. M. Raczkowski, R. Frésard, and A. M. Oleś, *Europhys. Lett.* **76** (2006) 128.
36. R. Frésard and M. Lamboley, *J. Low Temp. Phys.* **126** (2002) 1091.
37. G. Lhoutellier, R. Frésard, and A. M. Oleś, *Phys. Rev.* **B91** (2015) 224410.
38. R. Frésard and W. Zimmermann, *Phys. Rev.* **B58** (1998) 15288.
39. P.A. Igoshev, M.A. Timirgazin, V.F. Gilmutdinov, A.K. Arzhnikov, V.Yu. Irkhin, *J. Phys: Condensed Matter* **27** (2015) 446002.

10 *R. Frésard and V. H. Dao*

40. G. Kotliar, E. Lange, and M. J. Rozenberg, *Phys. Rev. Lett.* **84** (2000) 5180.
41. R. Frésard and K. Doll, Proc. of the NATO ARW *The Hubbard Model: Its Physics and Mathematical Physics*, eds. D. Baeriswyl, D. K. Campbell, J. M. P. Carmelo, F. Guinea, and E. Louis, San Sebastian (1993) (Plenum Press, 1995), p. 385.
42. N. Pavlenko and T. Kopp, *Phys. Rev. Lett.* **97** (2006) 187001.
43. W. Zimmermann, R. Frésard, and P. Wölfle, *Phys. Rev.* **B56** (1997) 10097.
44. R. Frésard and T. Kopp, *Nucl. Phys.* **B594** (2001) 769.
45. R. Frésard, H. Ouerdane, and T. Kopp, *Nucl. Phys.* **B785** (2007) 286.
46. R. Frésard and T. Kopp, *Ann. Phys. (Berlin)* **524** (2012) 175.
47. V. H. Dao and R. Frésard, *Ann. Phys. (Berlin)* **531** (2019) 1900491.
48. W. Metzner, and D. Vollhardt, *Phys. Rev. Lett.* **62** (1989) 324.
49. W. Metzner, *Z. Phys.* **B77** (1989) 253.
50. W. Metzner, and D. Vollhardt, *Phys. Rev.* **B37** (1988) 7382;
51. E. Müller-Hartmann, *Z. Phys.* **B74** (1989) 507.
52. D. Vollhardt, P. Wölfle, and P. W. Anderson, *Phys. Rev.* **B35** (1987) 6703.
53. V. H. Dao and R. Frésard, *Phys. Rev.* **B95** (2017) 165127.
54. A. Mezio and R. H. McKenzie, *Phys. Rev.* **B96** (2017) 035121.
55. K. Doll, M. Dzierzawa, R. Frésard, and P. Wölfle, *Z. Phys. B-Condens. Matter* **90** (1993) 297.